JOURNAL OF MATERIALS SCIENCE 21 (1986) 2651–2656

Fracture surface morphology of poly[*bis*(trifluoroethoxy)phosphazene]

M. KOJIMA
Chisso Corporation, 2-7-3 Marunouchi, Chiyoda-ku, Tokyo 100, Japan
J. H. MAGILL
Metallurgical and Materials Engineering Department, School of Engineering, University of Pittsburgh, Pittsburgh, Pennsylvania 15261, USA

Poly[*bis*(trifluoroethoxy)phosphazene] (PBFP) films were prepared from tetrahydrofuran solution. Fracture surface morphology was studied by scanning electron microscopy. Two morphologies associated with heat treatment have been established: (a) cospherically grown aggregates are obtained in solution-cast films and films heated through the $T(1)$ transition; (b) aggregates of irregular shaped crystalline platelets obtained after melting and crystallization. Ion etching was also applied to the fracture surface in order to clarify the morphological and structural features. The striations originally associated with the [*c*] axis direction of PBFP crystals can be accentuated on the fracture surface of original as-cast spherulitic films by employing this technique. The texture of the fracture surface after etching is compared with that obtained for an oriented fibre made from this polymer. From this comparison it can be concluded that the [*c*] axis direction is perpendicular to the spherulite radius. Furthermore the morphology is analogous in many respects to that of Kevlar.

1. Introduction

Within the last decade, investigations of physical properties of semicrystalline polyphosphazenes in regard to their molecular structure have been gradually developed [1–9]. Many kinds of phosphazene polymers have been prepared [10] and the semicrystalline nature of linear phosphazene homo-polymers has been established. Investigations of these polymers in our laboratories have focused on understanding the relationship which exists amongst morphology, structure and physical properties of these materials [11–18]. Solution-grown crystals and morphological features of some polyphosphazenes have been made and discussed. In addition, several crystal structures have been reported [11–17].

Mechanical behaviour such as creep [18] and dynamic moduli [6] have been studied while orientation density [6], ageing [18], thermal stability [19], and fire flammability [20] have also been investigated for selected polyphosphazenes. The spherulitic crystallization in PBFP thin films has been carried out and it has been established that the crystallite [*a*] axis direction lies predominantly along the spherulite radius with the [*c*] and [*b*] axis direction being oriented transversely with twisting non-cooperatively around the radius [16].

PBFP shows a mesomorphic transition designated as $T(1)$ near 90° C. The values of $T(1)$ depend upon the thermal history of the specimen [21]. Solution-cast spherulites comprised of chain-folded lamellae exhibit a $T(1)$ about 20 to 30° C lower, but are stabilized after heating specimens through this $T(1)$ transition to temperatures ranging upwards of the melting temperature [18].

The unit cell changes from a chain-folded α-orthorhombic modification to a pseudohexagnal modification upon passing into the thermotropic region, and then upon cooling to below $T(1)$, it reverts to a more stable γ-orthorhombic modification [17]. The purpose of the present paper is to extend this work to include morphological details of the PBFP spherulites. The effect of heat treatment on the spherulitic morphology in thick films, primarily studied by scanning electron microscopy, will be discussed.

2. Experimental techniques

2.1. Materials

Poly[*bis*(trifluoroethoxy)phosphazene] used in the present study was kindly provided by Drs G. Hagnauer and R. Singler of the Army Materials and Mechanics Research Center, Watertown, Massachusetts, U.S.A. The same materials has also been used in previous papers [11–18].

2.2. Spherulitic film preparation

Thicker spherulitic films were made by casting relatively concentrated polymer solution (several wt%) in tetrahydrofuran (THF) on to clean glass plates when the solvent was allowed to evaporate slowly at room temperature.

2.3. Heat treatment and fracture surface preparations

The films were sealed in the glass tube with nitrogen gas after previous evacuation of air. Heat treatment was carried out for specified times and temperatures as indicated in the figure captions. After heat

0022–2461/86 $03.00 + .12

treatment the films were fractured mechanically at room temperature for electron microscopy examination. Although the glass transition temperature of PBFP is reported [21] as low as -66°C, fracture occurs easily at room temperature in annealed specimens [18].

2.4. Scanning electron microscopy

The specimens for this examination were coated with Au/Pd alloy in a vacuum of about 30 Pa and subsequently examined with the JEOL JSM-T200 scanning electron microscope. X-ray diffraction measurement using Phillip's microbeam X-ray camera and Cu$K\alpha$ radiation were made at room temperature for crystal structure assignments.

2.5. Ion etching

In order to clarify the polymer texture, ion etching of the PBFP fracture surface was carried out using a JEOL JFC-1100 ion sputtering instrument operated at 500 V(AC) and 4 mA in air for a period of 1 h. The same chamber pressure and other conditions have been used successfully for etching other polymers [22, 23].

3. Results and discussion

The crystallization patterns observed for heat-treated spherulitic films of PBFP are complex [16]. Lath-shaped lamellar crystals of PBFP have been obtained from dilute THF/xylene solution (0.015 wt/vol % [11]. When the lath-shaped lamellar crystals are heated above $T(1)$, up to the melting temperature, T_m, the surface texture of these crystals is strongly affected by the heating conditions, but the overall shape (outline) of the crystals changes little after heating is carried out in this temperature range [10]. On the other hand, it has been observed optically that the overall spherulitic morphology of the PBFP films remains unaltered on heating through the $T(1)$ transition [24]. Note, however, that there is a change in the magnitude of the birefringence [18] (becomes more negative) on the first pass through the $T(1)$ region. Recently this transition has been examined in more detail [25].

Fig. 1 shows a scanning electron micrograph of the fracture surface of the PBFP spherulitic films as-cast from solution. Both X-ray and electron diffraction measurements of these thin films have established that the radius of the spherulites coincides with the crystallographic [c] axis of α-orthorhombic structure [16–18]. The morphological characteristics in Fig. 1 remain unaltered on heating specimens through $T(1)$ but still below T_m, as shown in Fig. 2, where the temperature was 150° C. The fibrillar nature of the spherulitic thin films has been noted by electron microscopy and described previously [16]. In Fig. 3 the fibrillar texture on the spherullite surface can be observed in the region (A) of this micrograph. PBFP morphology is comprised of well-defined lamellar crystalline platelets, typically 12 nm to 15 nm thick. These have been made by crystallizing the polymer from a dilute (0.15 wt/vol %) mixed solution of THF and xylene. An electron diffraction pattern of these crystals demonstrates that the reflections occur only from ($h\,k\,0$) crystal planes [11, 12] so that the platelets must be comprised of folded-chain molecules in arrays perpendicular to the broad crystalline platelet surface. The spherulites are comprised of lamellar crystalline platelets akin to those encountered in conventional organic semi-crystalline polymers, such as high-density polyethylene, isotactic polypropylene.

Fig. 4 shows a scanning electron micrograph which indicates three differently oriented regions of texture

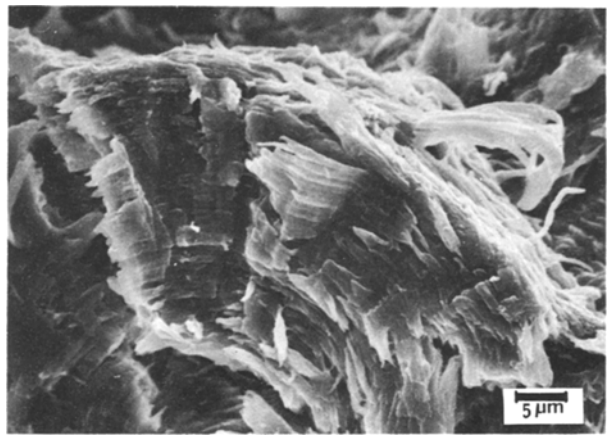

Figure 2 Fracture surface of the solution-cast PBFP spherulitic film which was heated at 150° C for 60 min and then cooled to room temperature slowly.

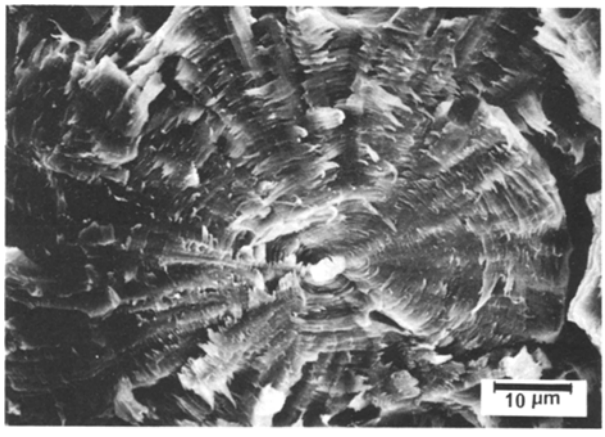

Figure 1 Scanning electron micrograph of a fracture surface of a PBFP spherulitic film cast from concentration THF solution.

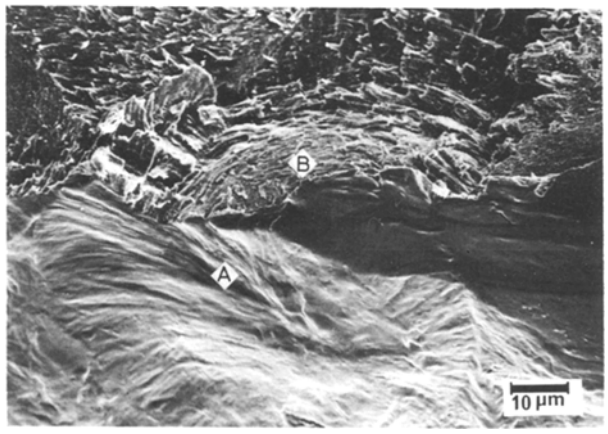

Figure 3 Morphology of the PBFP cast film: (a) fracture surface, B, and (b) free surface, A.

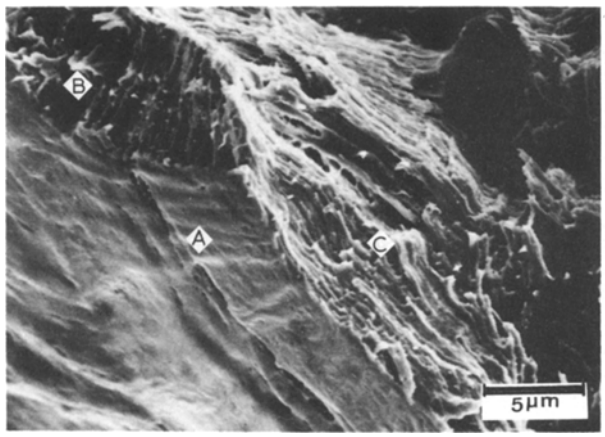

Figure 4 Scanning electron micrograph of the PBFP cast film shows three different features: A, free surface; B, perpendicular to the spherulite radius; and C, parallel to the spherulite radius.

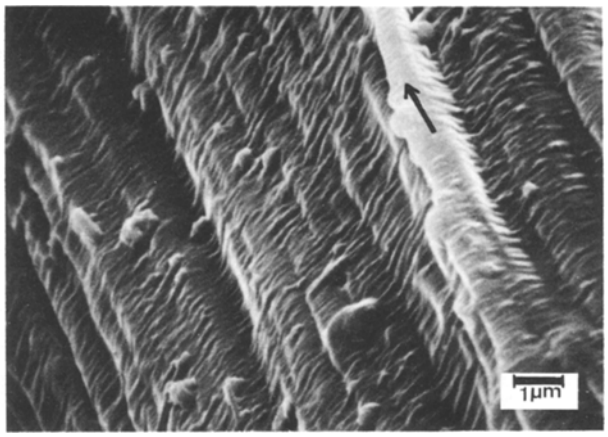

Figure 6 Scanning electron micrograph of an ion-bombarded PBFP fibre surface. The arrow shows the draw direction.

across the PBFP spherulites, i.e. the spherulite surface (A), and fracture surface perpendicular (B) and then a region (C) parallel to the spherulite radius direction, respectively. Although the fibrillar nature is not clearly defined in this micrograph, because of an unsuitable angle for the SEM observation, the fibrillar regions appear like the intersection of crystalline platelets with the spherulite surface. In general, it is noted that the growth front of three-dimensionally grown PBFP spherulites is textureless and we do not understand this featureless aspect of the PBFP spherulite growth surface. Note, too, that the fracture surface morphology remains unaltered after the specimen is heated and cooled through the $T(1)$ region. However, the phase transformation from α-orthorhombic to γ-orthorhombic after heating at temperatures between $T(1)$ and T_m has been well established by X-ray diffraction measurements on THF solution-cast PBFP specimens [17].

The differences in sample toughness between unheated and heated specimens must be associated with changes in the morphology. As extended-chain crystals form upon passing through the mesophase, the toughness in the lateral direction (intermolecularly) in the specimen decreases after this heat treatment [10]. Figs 1 to 3 illustrate the growth morphology in PBFP spherulites where fracture occurs in two modes in these micrographs namely: (a) where most of spherulites are fractured along the spherulite radius; and (b) as seen in region B in Fig. 3 and where fracture occurs tangentially along the spherulite surface. These fracture features mean that the PBFP spherulites are comprised of cospherical aggregates of crystals less than 1 μm thick. Fig. 5 illustrates the fracture surface morphology of PBFP spherulites in solution-cast films after ion bombardment. Again, the cospherical arrays of platelets found in unetched surfaces (Fig. 1) become more visible after etching when arrays of striations within the platelets and perpendicular to the spherulite radius, can be seen clearly (see the arrow in Fig. 5). It is interesting to note that when the drawn fibre of PBFP is ion-etched as in Fig. 5, arrays of similar striations are noted to extend perpendicular to the draw direction (see the arrow in Fig. 6). Related morphological features such as these have been noted in highly drawn ion-etched conventional organic semicrystalline polymers where the lamellae always appear to be oriented perpendicular to a [c] axis of polymer crystals [22, 23]. In Fig. 7, region A shows an array of striations caused by etching, but region B does not show such texture on the same ion-etched fracture surface. When the fracture occurs perpendicular to the cospherically arrayed platelets, or makes an angle with the [c] axis direction, it is possible to observe a non-layered almost textureless fracture surface

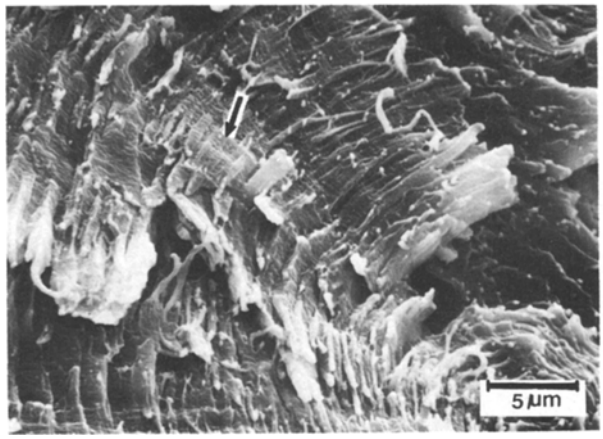

Figure 5 Ion-bombarded (etched) fracture surface morphology of THF solution-cast PBFP film.

Figure 7 Ion-bombarded fracture surface morphology of the THF solution-cast PBFP film.

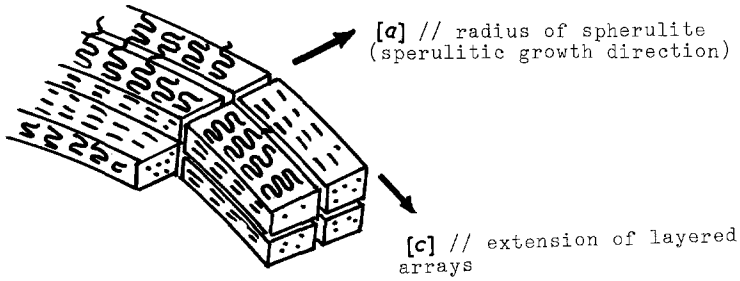

Figure 8 Schematic representation of the surface morphology in solution-cast PBFP spherulitic aggregates. Crystallographic axis directions are included.

morphology. Such observations indicate that the striated texture noted in PBFP specimens is not an artefact introduced during specimen preparation and manipulation.

The relationship between the morphology and the crystallographic axis direction is clarified in the illustration of the ion-etched fracture surface of solution-grown spherulitic PBFP in Fig. 8. When molecular chains are so arranged, fibrillation takes place easily along the direction of the radius between adjacent platelets as seen in Fig. 5. Fracture occurs predominantly parallel to a plane which includes the [*c*] axis. The platelets are estimated to be 10 μm or more in length in the tangential direction and 2 to 3 μm in the radial direction of the spherulites. These overall morphological features in as-cast PBFP spherulitic films are retained through the $T(1)$ transition and up to melting temperature. However, after specimens are melted and then cooled to room temperature, a new fracture texture obtains. Fig. 9, illustrates this new fracture morphology after the specimen was melted in a sealed glass tube with nitrogen gas at 250° C for 5 min and then cooled quickly to 70° C, where it was kept for 28.5 h before its examination at room temperature. The fracture surface does not show the usual spherulitic feature, but it now consists of thicker lamellar aggregates with broad platelets often emanating from a common nucleus or centre as seen in this and later micrographs.

Fig. 10 shows the surface morphology of PBFP spherulites obtained from the melt in the same manner as in Fig. 9. The spherulite surface is comprised of thin layered platelets irregularly stacked, which differ from those of the unmelted specimens. Surface fracture features are enhanced by ion etching (see Figs 11a and b) for example in a specimen quenched in liquid nitrogen after melting at 250° C for 5 min. After fracturing and ion-etching, the specimen is often wrinkled at right angles to [*c*] axis direction, although it is not so clearly shown in Fig. 11b.

In other ion-etched fracture surfaces, arrays of irregularly framed broad platelets are also shown in Fig. 11a. The scanning electron micrograph of an ion bombarded surface (Fig. 11c) shows voids created inside the specimen already shown in Fig. 9. The striations show irregularies on the etched surface in Fig. 11c. Sometimes these void surface regions are strongly affected by ion bombardment and so layers of approximately the same thickness as the platelets in Fig. 11b (arrowed) are formed. Fig. 11d is a scanning electron micrograph of ion-etched fracture surface – the counterpart was shown in Fig. 9. From the direction of the striations on the platelets it is deduced that the [*c*] axis direction lies parallel to the long direction of the platelets, arrowed in Fig. 11d and similar to the example shown in Fig. 6. Striations seen in Fig. 11d appear to be irregular and may be associated with extended-chain molecules formed in the mesophase region during cooling from the melt. The melt to mesophase morphology nucleates and grows rapidly above 230° C but three-dimensional order does not develop until $T(1)$ is traversed upon cooling.

In some respects the banded morphology of PBFP is similar to that of Kevlar where cleavage occurs (after chemical etching [26]) at right angles to the fibre axis. Analogously too (Fig. 12), ragged ends are produced whenever unetched highly oriented polymers, such as PBFP or poly(*bis*phenoxyphosphazene) (PBPP), are torn or broken through stretching. The concentric lamellar-like texture of PBFP in Fig. 1 of

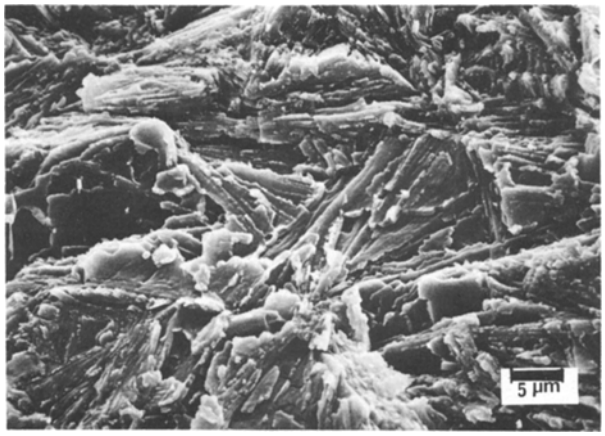

Figure 9 Room-temperature fracture surface morphology of PBFP specimen isothermally heated in nitrogen at 70° C for 28.5 h after fusion at 250° C (5 min).

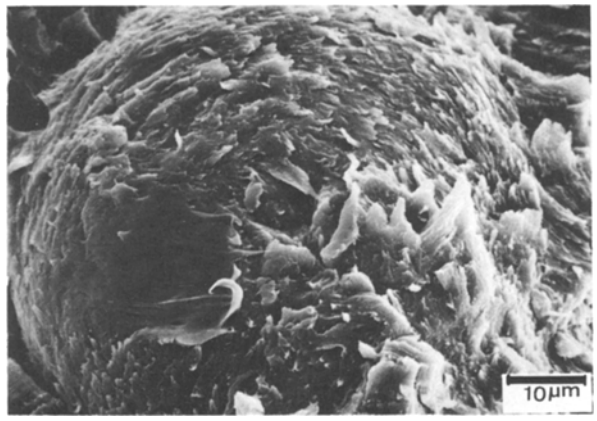

Figure 10 Surface morphology of PBFP spherulite obtained from the melt by crystallizing at 70° C for 28.5 h.

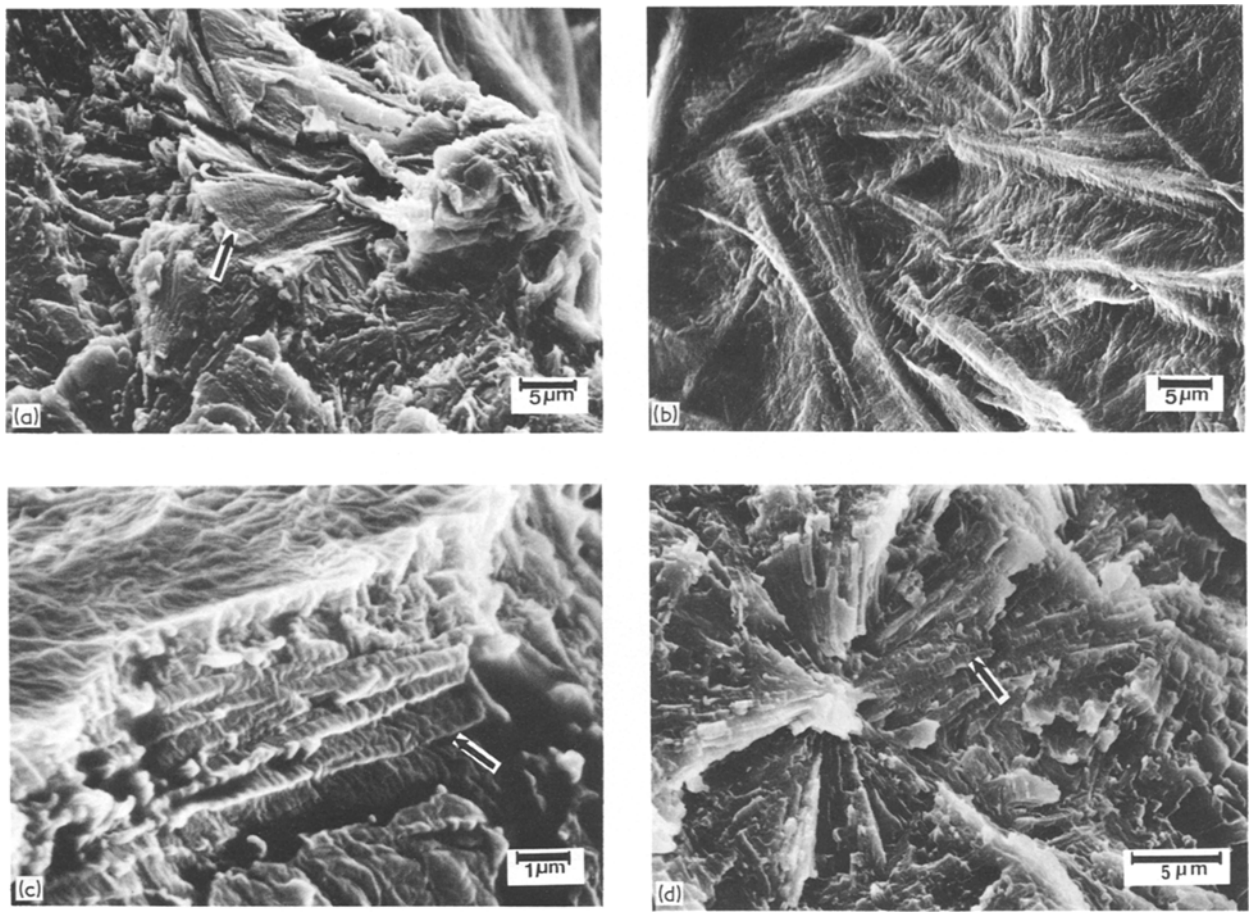

Figure 11 (a) and (b) Ion-bombarded fracture surface morphology of PBFP quenched to liquid nitrogen from the melt. (c) Free surface of a void created inside the specimen. (d) The arrow shows the striation.

[26] and Figs 1, 2 and 5 of this text, where spherulites and fibres of PBFP are displayed, is noteworthy. Topological defects and voids are well known in Kevlar [27], ultra highly oriented polyethylene [28] (UHMWPE), and in polyacetylene [29] whiskers for example, all of which when etched chemically, develop circumferential cracks from existing surface flaws. It appears that in all of these well-oriented linear polymers, that relatively weak interchain (cohesive) bonding exists as within the PBFP spherulites, comprised of strata of cospherical shells about 1 μm thick layers. These appear to undergo cleavage in two directions. The failure directions in PBFP fibres, ion etched, unetched and annealed too, are now being investigated in regard to their morphology–strength behaviour in these highly crystalline polymers [30] formed from the mesophase or crystallized from the melt.

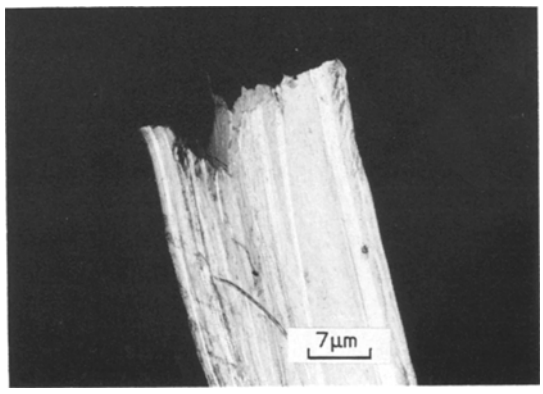

Figure 12 Optical micrograph (crossed-polars) of a fractured film of poly(*bis*phenoxyphosphazene) drawn at room temperature.

4. Conclusion

From the fracture surface morphologies of PBFP films studies by scanning electron microscopy, it has been established that:

1. solution cast spherulitic aggregates of PBFP consist of cospherical platelets;
2. the cospherical morphology does not appear to alter upon heating the PBFP through $T(1)$ transition up to below T_m, even though the discrete long period disappears about $T(1)$;
3. recrystallization from the melt gives rise to broad plate-like crystals which differ in size from the spherulitic morphology in the solution-cast films;
4. the striations in the [c] axis direction associated with the fracture surface of the original spherulitic films can be highlighted by ion bombardment;
5. cospherical aggregates grow with the [c] axis oriented tangentially along the spherulite surface;
6. the morphology of PBFP and PPT (Kevlar) seem to be related.

Acknowledgement

We are most grateful to Drs G. Hagnauer and R. Singler of AMMRC for supplying the polyphosphazene used in this investigation. We wish to express our thanks to Mr H. Satake for his assistance in the electron microscopy. Support was provided in part by the National Science Foundation, Polymer Program.

References

1. D. P. TATE, *J. Poly. Sci. Polym. Symp. Ed.* **40** (1974) 33.
2. P. J. LIEU, J. H. MAGILL and Y. C. ALARIE, *J. Combust. Toxicol.* **7** (1980) 143.
3. *Idem, ibid.* **8** (1981) 242.
4. E. J. QUINN and R. L. DIECK, *J. Fire Flammability* **7** (1976) 358.
5. *Idem, ibid.* **8** (1977) 412.
6. I. C. CHOY and J. H. MAGILL, *J. Appl. Polym. Sci.* **19** (1981) 2495.
7. A. K. CHATTOPADHAY, R. L. HINRICKS and S. H. ROSE, *J. Coatings Technol.* **51** (1979) 87.
8. R. E. SINGLER, N. S. SCHNEIDER and G. L. HAGNAUER, *Polym. Eng. Sci.* **15** (1975) 34.
9. S. J. KOZMISKI and I. R. HARRISON, *J. Appl. Polym. Sci.* **27** (1982) 1783.
10. H. R. ALLCOK, *Makromol. Chem. Suppl.* **4** (1983) 4.
11. M. KOJIMA and J. H. MAGILL, *Polymer Commun.* **24** (1983) 329.
12. M. KOJIMA, W. KLUGE and J. H. MAGILL, *Macromolecules* **17** (1984) 1421.
13. M. KOJIMA and J. H. MAGILL, Paper presented at the American Physical Society, (DHPP) Abstracts No. MT4, P561 and BT4, p. 283, Detroit, Michigan, 26 to 30 March (1984).
14. M. KOJIMA, J. H. MAGILL and T. MASUKO, *Polym Preprints* Jpn. **33** (1984) 2259.
15. M. KOJIMA and J. H. MAGILL, *Polymer Commun.* **25** (1984) 273.
16. *Idem, Polymer* **26** (1985) 1971.
17. *Idem, Makromol. Chem.* **18** (6) (1985) 649.
18. T. MASUKO, R. L. SIMEONE, J. H. MAGILL and D. J. PLAZEK, *Macromolecules* **17** (1984) 1471.
19. S. V. PEDDADA and J. H. MAGILL, *ibid.* **16** (1983) 1258.
20. *Idem, J. Fire Flammability* **11** (1980) 63.
21. N. S. SCHNEIDER, C. R. DESPER and J. J. BERES, Mesomorphic Structure in Polyphosphazenes, in "Liquid Crystalline Order in Polymers", (Academic, New York, 1978) pp. 299–325.
22. M. KOJIMA and H. SATAKE, *J. Polym. Sci. Polym. Phys. Ed.* **20** (1982) 2153.
23. *Idem, ibid.* **22** (1984) 285.
24. G. ALLEN, C. J. LEWIS and S. M. TODD, *Polymer* **11** (1979) 44.
25. J. H. MAGILL, J. PETERMANN and U. RIECK, paper presented at the Frühjahrstagung, Lausanne, 18 to 20 March (1985); *Colloid Polym. Sci.* in press.
26. M. HORIO, T. KANEDA, S. ISHIKAWA and K. SHIMAMURA, *J. Soc. Fiber Sci. Technol.* **40** (1984) T285.
27. M. G. DOBBS and J. E. McINTYRE, *Adv. Polym. Sci.* (1984) 61.
28. J. SMOOK, W. HAMERSMA and A. J. PENNINGS, *J. Mater. Sci.* **19** (1984) 1359.
29. D. N. BATCHELDER, G. CALOITIS, R. T. READ and K. J. YOUNG, Proceedings of the Conference on Deformation, Yield and Fracture of Polymers, Cambridge, (1982) p. 21.
30. J. H. MAGILL, M. KOJIMA and G. McMANUS, unpublished results.

Received 30 April
and accepted 4 July 1985